# Numerical Study of Power Deposition, Transport and Acceleration Phenomena in Helicon Plasma Thrusters

M. Magarotto, M. Manente, P. de Calro, F. Trezzolani, D. Pavarin, and D. Melazzi
*CISAS, Padova, Italy*

**Abstract: We want to develop a numerical model of an Helicon Plasma Thruster. In particular the production stage, namely the plasma source, has been modeled with a fluid solver implemented in OpenFOAM which solves for the plasma transport, coupled to the Electro Magnetic solver ADAMANT which solves for the power deposition. The acceleration stage, namely the plasma plume, has been studied with F3MPIC, a full 3D Particle-In-Cell code coupled to an electro static solver implemented in GetDP. The proper boundary conditions to couple the production stage and the acceleration stage tools is still under revision. We have studied two cylindrical plasma sources respectively with a 1D and a 3D version of the fluid solver we have implemented in OpenFOAM. Even though the power deposition profile has been assumed and not calculated, we have predicted the main features of a cylindrical plasma source, e.g. plasma density peak in the center of the discharge. We have compared our results against the commercial software COMSOL Multiphysics ®, the agreement between the two codes is good (differences lower than $< 1\%$).**

## I. Introduction

Recent advances in plasma-based propulsion systems have led to the development of Helicon Plasma Thrusters[1] (HPTs), whose plasma-generation system is derived from high-density Helicon plasma sources.[2] Helicon source is capable of depositing electromagnetic power efficiently creating very dense plasma; this efficient plasma generation can lead to high specific impulses and good thrust efficiency. In HPTs (see Figure 1) we can distinguish between two main stages: the production stage where plasma is generated through a Helicon source, and the acceleration stage where divergent magnetic field lines provide a magnetic nozzle effect. The main components of the production stage are a gas feeding system, a RF antenna and magnetic coils. In the production stage neutral gas is injected into a dielectric cylinder and ionized by the RF antenna system working in the MHz range; the magnetic coils provide the quasi-axial magnetic field that allows for both the confinement of the plasma and the propagation of whistler waves.[3] The acceleration stage is realized through the divergent magnetic field lines at the exhaust section which provide a magnetic nozzle

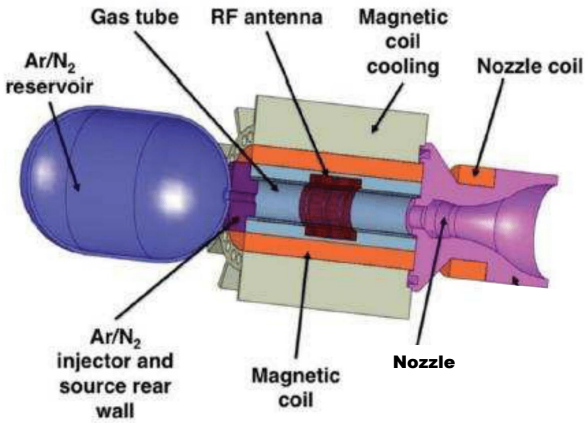


**Figure 1. Helicon Plasma Thruster Scheme.**

effect on the magnetized plasma. Some of the main projects that are developing HPTs are: the high-power VASIMR[4] where a first-stage Helicon source is coupled to a second-stage ion cyclotron resonance heating for ion heating; the Australian project developed by ANU[5] that aims at developing medium power HPT; the Europeans HPH.COM[6] based on a low power ($\leq$100 W) Helicon source, and SAPERE-STRONG[7] based on an high power ($\geq$1 KW) Helicon source.

In HPTs the propulsive figures of merit (e.g., specific impulse and thrust) are strictly related to the power deposited by the RF antenna into the Helicon source (and the plasma transport therein), and to the acceleration process at the exhaust. Therefore, in order to perform the design and possibly the optimization of HPTs, we need theoretical and numerical models for both the production and the acceleration stages. Standard numerical approaches rely on Electro-Magnetic (EM) simulations coupled to either kinetic or Particle-in-Cell (PIC) strategies to reproduce the plasma response in both stages.[8–10] However in HPTs that employ an high-power plasma source (e.g. SAPERE-STRONG) the plasma density can reach values higher than $> 10^{19}$ m$^{-3}$; such values cannot be handled by a PIC code, while could result in a computational burden for a kinetic approach. The numerical simulation strategy adopted in our group consists on reproducing: i) the plasma transport in a high-power plasma source with a fluid strategy so as to keep the computational cost at bay; ii) the plasma acceleration and detachment with a PIC strategy, in fact in the acceleration stage the lower plasma density allows for the employment of a PIC tool with a reasonable calculation time.

Wave propagation and plasma transport are respectively solved by means of ADAMANT,[11] and a fluid solver;[12] both solvers are coupled in an iterative loop. The fluid solver has been implemented in OpenFOAM,[13] an open source C++ library which solves differential problems with the Finite Volume Method (FVM). OpenFOAM is designed for solving 3D problems and defines all meshes as such; however, 1D and 2D problems can be simulated by generating a mesh in 3D and applying special boundary conditions.

The acceleration stage is studied through F3MPIC,[10] a plasma PIC code coupled with a finite element electrostatic solver in time domain. F3MPIC has been validated and widely employed during the HPH.COM project.[6] We opted for classical PIC strategy even though both fluid[14] and hybrid codes[15] have been proposed in order to study the plasma plume. Fluid codes, although fast and reliable, present some critical issues:[14] i) in the region near the thruster outlet (some thruster radii) phenomena such as charge-exchange must be handled only with a kinetic approach; ii) in the far region, where the plasma is quasi-collisionless, Electron Energy Distribution Function (EEDF) must be assumed. Also hybrid codes (electron-fluid and ions-PIC) have the drawback that EEDF must be assumed, in fact EEDF can be far from Maxwellian if Double Layer (DL) arises in the plasma plume.[16] DL simulation is a critical task because: i) DL role on propulsive performances[5] is still debated; ii) there is not a complete agreement on the nature of DL that arises in HPTs, hence on the assumptions that can be done on EEDF.[15,16] Therefore, for sake of generality, we have resorted on a full PIC strategy for plume modeling.

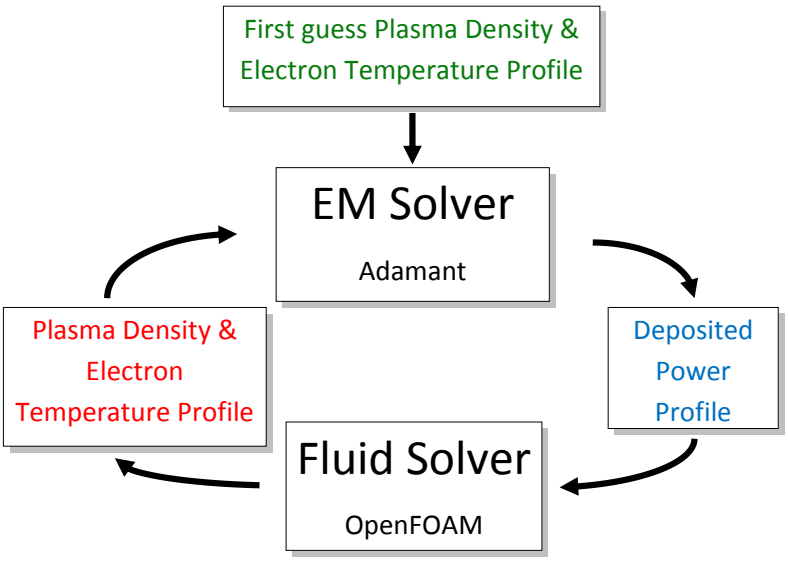


**Figure 2. Source stage numerical tool scheme.**

In section II we will describe more throughly the coupling strategy between ADAMANT and OpenFOAM (which constitute the source stage solver), the F3MPIC code (which constitute the acceleration stage solver), and the coupling between the source stage solver and the acceleration stage solver. In section III we will describe the model implemented in the fluid solver and results obtained with the same tool operated singularly, i.e. not coupled to the EM solver nor to the acceleration stage. In particular we have studied two cylindrical plasma sources respectively with the 1D and the 3D versions of our fluid solver; in the 1D simulation we have studied the inhomogeneities of plasma parameters profiles only along the axial direction of the plasma source, while in the 3D case we have accounted for the plasma inhomogeneities in every direction. In addition we have compared our results against the commercial software COMSOL Multiphysics ®[17] which solves differential problems with Finite Element Methods (FEM).

## II. Methodology

In order to model the Helicon production stage we have to account for the coupling of the wave propagation and the plasma transport; this can be done studying the two phenomena with two dedicated tools run iteratively (see Figure 2). This approach is justified because the time scaling at which the two phenomena happen is different: the wave propagation is by far faster than the plasma diffusion. In the study of the plasma transport, the wave propagation can be retained as a source term through the power deposited by the antenna into the plasma; in the solution of the wave propagation, the plasma parameters can be considered at the equilibrium.

The thruster acceleration stage has been modeled with F3MPIC, a three-dimensional plasma Particle-in-Cell code coupled with a 3D electrostatic and electromagnetic solver in time domain implemented in the FEM tool GetDP.[18] F3MPIC relies on an unstructured tetrahedra mesh, therefore geometries of arbitrary shape and complexity can be managed. The code evaluates the charged particles trajectories of a multiple species plasmas with a Boris-Leapfrog scheme[19] under the reaction of electromagnetic fields generated by the plasma itself and by other external sources. An arbitrary number of charged species can be treated. Both plasma and non-plasma regions can be managed. At each time step, charge and current densities on nodes of the unstructured mesh are obtained by means of appropriate weighting schemes.[10]

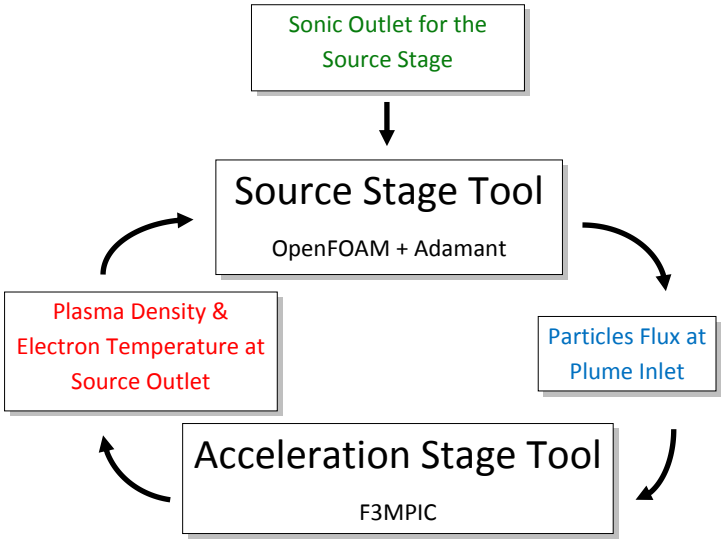


**Figure 3. Entire thruster simulation strategy scheme.**

In order to couple the source stage and the acceleration stage tools we have to find the proper boundary conditions at the source outlet, i.e. at the plume inlet. This matching condition is found iteratively (see Figure 3): i) the particles flux at the source outlet, calculated with the fluid code, is the boundary condition for the PIC code at the plume inlet; ii) vice versa the plasma parameters profile (e.g. plasma density and electron temperature), predicted by the PIC code, are the boundary conditions for the fluid code at

the source outlet. In Ahedo[20] the boundary condition at the plume inlet derives from the particles flux calculated with a source model which assumes sonic outlet. This hypothesis will be employed to initialize the iterative loop between source stage and acceleration stage tools. The iteration process will be concluded at the achievement of the matching boundary condition.

## III. Fluid Model

### A. Model Description

Plasma is considered as a multi-fluid mixture composed of electrons, ions, neutrals and excited. Electron density $n_e$ and electron energy $n_\varepsilon$ are solved through the drift-diffusion[21] approximated continuity and energy equations. Ion $n_i$, neutral $n_0$ and excited $n_s$ density are solved through the drift-diffusion form of the continuity equations (ion, neutral and excited temperature are assumed equal to the initial gas temperature $T_0$). An electrostatics model is employed to compute the plasma potential $\phi$.

The $k$-th species number density $n_k$ is calculated with the continuity equation

$$\frac{\partial n_k}{\partial t} + \nabla \cdot \mathbf{\Gamma}_k = R_k \tag{1}$$

where $\mathbf{\Gamma}_k$ is the flux vector and $R_k$ is the particles source term. The flux vector is given by the drift diffusion approximation $\mathbf{\Gamma}_k = n_k \mathbf{v}_k = \pm \mu_k n_k \mathbf{E} - D_k \nabla n_k$, where $\mathbf{v}_k$ is the species velocity, $\mathbf{E}$ is the electrostatic field, $D_k$ the species diffusivity, and $\mu_k$ the species mobility. The electron energy density is calculated from the energy equation

$$\frac{\partial n_\varepsilon}{\partial t} + \nabla \cdot \mathbf{\Gamma}_\varepsilon + \mathbf{E} \cdot \mathbf{\Gamma}_e = R_\varepsilon \tag{2}$$

where $\mathbf{\Gamma}_\varepsilon$ is the energy flux vector and $R_\varepsilon$ is the energy source term. In the drift diffusion approximation the energy flux vector reads $\mathbf{\Gamma}_\varepsilon = -\mu_\varepsilon n_\varepsilon \mathbf{E} - D_\varepsilon \nabla n_\varepsilon$, where $\mu_\varepsilon$ is electron energy mobility and $D_\varepsilon$ is the diffusion energy mobility. The electrostatic potential is calculated via the Poisson equation

$$\nabla^2 \phi = -\frac{n_i - n_e}{\varepsilon_0} \tag{3}$$

where $\varepsilon_0$ is the vacuum permittivity.

We have considered an Ar discharge characterized by three electron impact reactions, namely elastic scattering, ionization and excitation. The reaction rate constants for these three reactions can be calculated, in function of the electron temperature $T_e$, following the empirical relations reported by Libermann and Lichtenberg.[22] The ion $Ar^+$ diffusion properties are calculated interpolating the experimental data reported by Chicheportiche.[23]

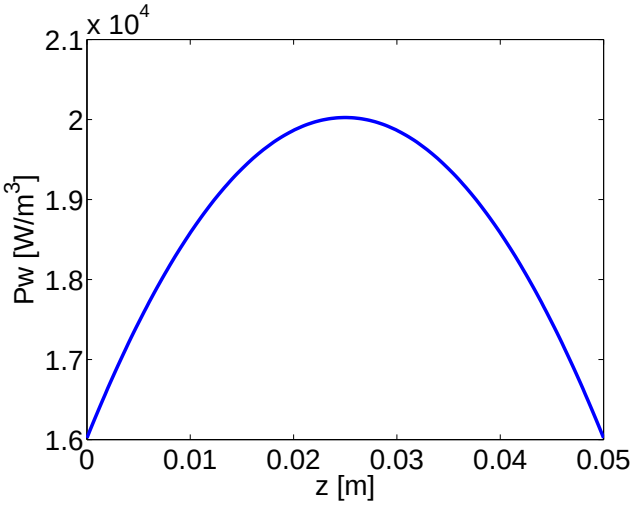


**Figure 4.** ***1D case*: assumed power deposition profile Pw, expressed in function of the position.**

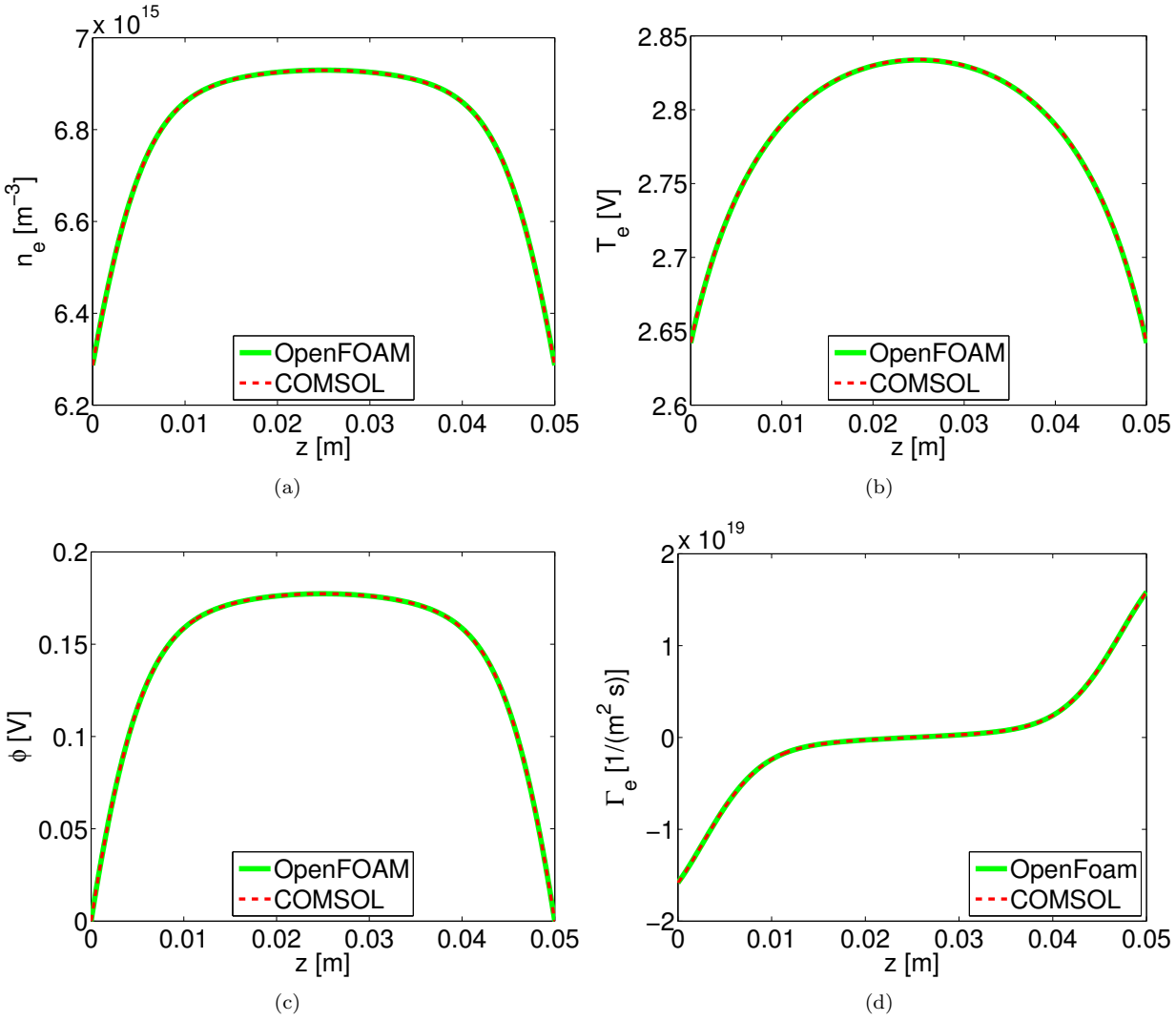


**Figure 5.** *1D case*: **a) plasma density $n_e$, b) electron temperature $T_e$, c) electrostatic potential $\phi$, d) electron flux density $\Gamma_e$ in function of the position. The results of our solver (OpenFOAM) have been compared with the solution of the commercial software COMSOL. Initial neutral number density $n_0 = 10^{22}$ m$^{-3}$; power deposition profile as reported in Figure 4. Results at instant $t = 10^{-7}$ s, assumed uniform initial conditions $n_{e0} = 6.24 \times 10^{15}$ m$^{-3}$, $T_{e0} = 3$ eV, $\phi_0 = 0$ V.**

The electron and ion boundary condition is given by the Bohm sheath criterion.[22] The neutrals boundary condition are determined assuming that all the ions and excited colliding against the wall recombine; therefore the neutral particles flux $\Gamma_0 = -(\Gamma_i + \Gamma_s)$. The electron energy boundary condition is imposed in accordance with Mikellides.[24] The grounded walls is the boundary condition for the Poisson equation $\phi = 0$.

## B. Results

We have studied two cylindrical plasma sources respectively with a 1D formulation of the fluid problem (only axial gradients accounted) and with a 3D formulation. Hereinafter the two situations will be referred as to *Case 1D* and *Case 3D*. In both cases we have compared the results of our solver against the commercial software COMSOL Multiphysics ®, in which we have implemented the same fluid model of our solver.

### 1. *Case 1D*

The cylindrical plasma source analyzed has radius $R = 0.0056$ m, and length $L = 0.05$ m. Provided that the results here presented concerns only the fluid solver run singularly, nor coupled to the EM solver, we had to assume a power deposition profile; we opted for the one reported in Figure 4. The initial neutral number density is $n_0 = 10^{22}$ m$^{-3}$. The other initial conditions are uniform profiles of electron number density $n_{e0} = 6.24 \times 10^{15}$ m$^{-3}$, electron temperature $T_{e0} = 3$ eV, and electrostatic potential $\phi_0 = 0$ V. In particular the results reported in Figure 5 are relative to the simulation stopped at the instant $t = 10^{-7}$ s, namely when the equilibrium condition is not achieved yet.

Even thought not at the equilibrium we can identify some expected features: a) the electron number density $n_e$ is peaked in the center of the discharge, b) the electron temperature is higher in correspondence

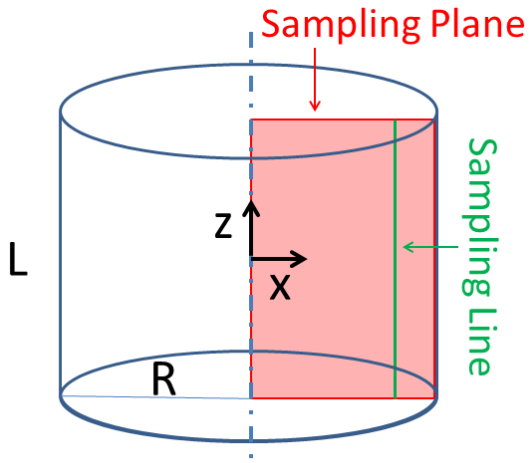


**Figure 6.** ***3D case*: sketch of the cylindrical plasma source. Cylinder radius R = 0.005 m, cylinder length L = 0.005 m. Our tool results will be presented on the *Sampling Plane*, the semi-plane in which $0 \leq x \leq R$, and $-L/2 \leq z \leq L/2$. The comparison between our solver and COMSOL has been performed along the *Sampling Line*, which is the line in the *Sampling Plane* for x = 3/4R.**

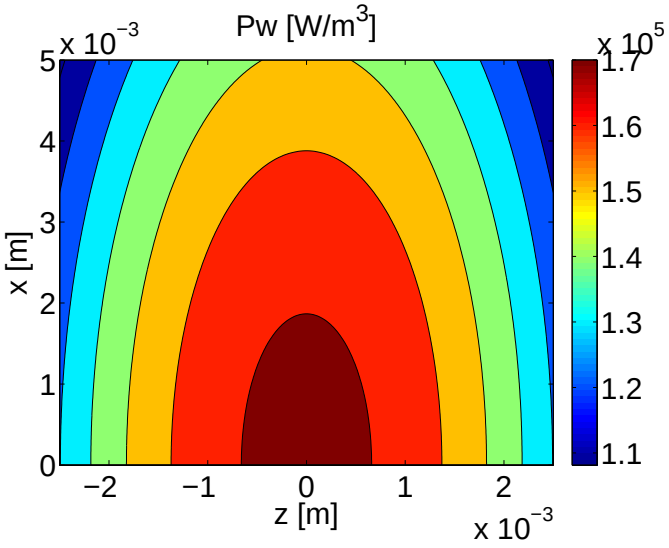


**Figure 7.** ***3D case*: assumed power deposition profile Pw, expressed in function of the position and reported on the *Sampling Plane*.**

of the deposited power peak, c) the electrostatic potential is positive in the plasma bulk, d) the electron flux is higher near the source walls and directed against the boundary of the source. In addition we can notice a very good agreement between our results (implemented in OpenFOAM), and the results obtained with COMSOL; more specifically this really good agreement is obtained for an intermediate instant of the simulation, and not only when convergence is achieved.

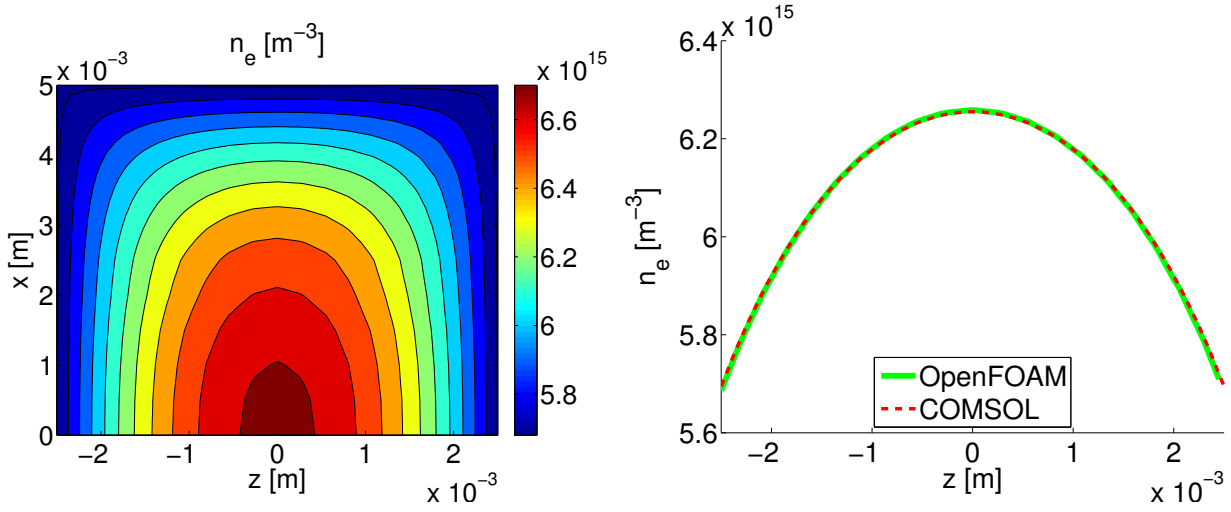


(a) (b)

**Figure 8.** ***3D case*, plasma density $n_e$ in function of the position: a) our solver output in the *Sampling Plane*, b) comparison between our solver and COMSOL results along the *Sampling Line*. Initial neutral number density $n_0 = 10^{21}$ m$^{-3}$; power deposition profile as reported in Figure .**

### *2. Case 3D*

The cylindrical plasma source analyzed has radius $R = 0.005$ m, and length $L = 0.005$ m. Being the geometry studied 3D, we have chosen to present the estimated plasma parameters on a *Sampling Plane* (see Figure 6), namely a semi-plane which include the axis of the cylinder. More precisely the results will be presented in the region where $0 \leq x \leq R$, and $-L/2 \leq z \leq L/2$. We have also identified a *Sampling Line* over which our results have been compared against COMSOL. The *Sampling Line* is included in the *Sampling Plane* and is put in correspondence of $x = 3/4R$.

We have assumed the power deposition profile reported in Figure 9; the initial neutral number density is $n_0 = 10^{21}$ m$^{-3}$; the simulation has been run until the convergence.

We can identify some expected features: a) the electron number density $n_e$ is peaked in the center of the discharge (see Figure 8a), b) the electron temperature is higher in correspondence of the deposited power peak (see Figure 9a). In addition being both the geometry and the power deposition profile axisymmetric both $n_e$ and $T_e$ are so; therefore the results presented in the *Sampling Plane* are enough to give a complete description of the source. The comparison against COMSOL on the *Sampling Line* has been reported in Figure 8b and Figure 9b respectively for $n_e$ and $T_e$. The agreement between the two solvers is good with differences lower than 1%, justified by the different methods applied in the two solvers: OpenFOAM adopt FVM, COMSOL adopt FEM.

## IV. Conclusion & Future Work

We have analyzed two cylindrical plasma sources respectively with a 1D (only axial gradients evaluated) and a full 3D version of the fluid solver implemented in OpenFOAM. Even though the power deposition profile has been assumed, we have predicted the main features of a cylindrical plasma source: i) plasma density peak in the center of the source, ii) temperature peak in correspondence of the power deposition profile peak. In addition we have validated the results of our tool against COMSOL for both the 1D and the 3D simulation cases. We have implemented in COMSOL the same physical model of our solver and the

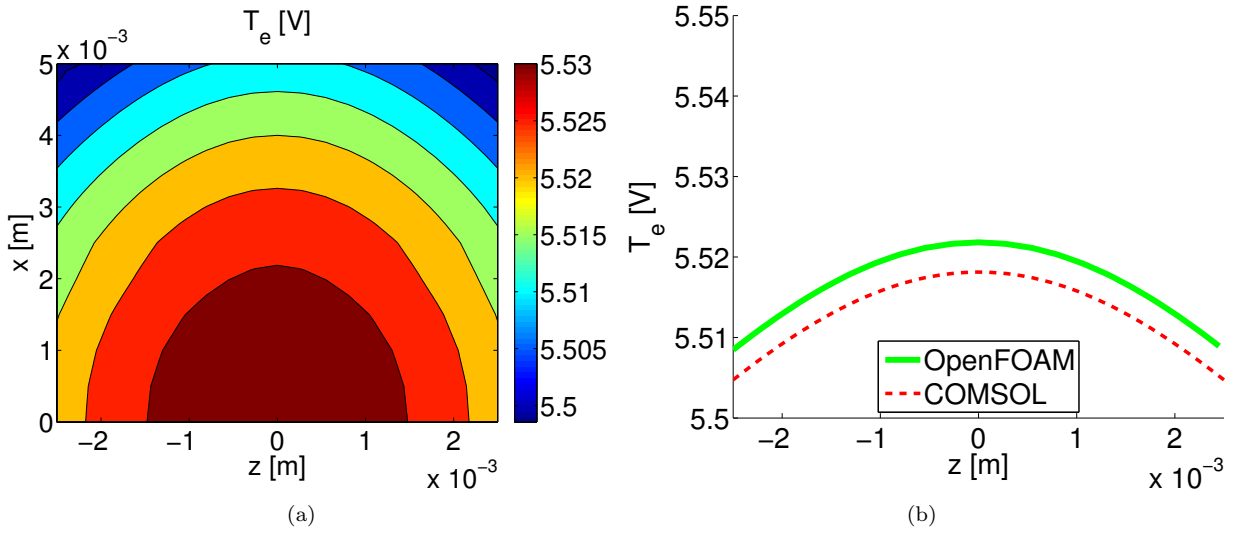


(a) (b)

**Figure 9.** ***3D case*****, plasma density $T_e$ in function of the position: a) our solver output in the** ***Sampling Plane*****, b) comparison between our solver and COMSOL results along the** ***Sampling Line*****. Initial neutral number density $n_0 = 10^{21}$ m$^{-3}$; power deposition profile as reported in Figure .**

two tool have shown a very good agreement (differences lower than $< 1\%$).

All the numerical tools employed in the simulation of the thruster, namely the fluid and EM solvers for the plasma source modeling and the PIC tool for the plume modeling, have been validated in this and previous works.[10–12] Therefore the next step of our work will be to couple the fluid and the PIC codes, in order to describe the overall dynamic of the thruster.

## References


[1]Pavarin, Daniele, et al. "Design of 50 W helicon plasma thruster." *31st Int. Electric Propulsion Conf.*, Ann Arbor, MI. 2009.

[2]Chen, F. F., "Helicon plasma sources", *High Density Plasma Sources*, 1995, pp. 1–75.

[3]Chen, F. F., and Arnush, D., "Generalized theory of helicon waves I. Normal modes", *Phys. Plasmas*, Vol. 4, No. 9, 1997, pp. 3411–3421.

[4]Chang Diaz, F. R., "The Vasimir", *Sci. Am.*, Vol. 283, No. 5, November 2000, pp. 90–97.

[5]Charles, C., et al., "Helicon double layer thrusters", *Proc. 27th Int. Conf. on Phenomena in Ionized Gases*, Eindhoven, 2005.

[6]Pavarin, D., et al., "Helicon Plasma Hydrazine Combined Micro Project Overview and Development Status", *Proceedings of the Space Propulsion Conference*, San Sebastian, Spain, 2010.

[7]Mazari Villanova, L., Papi L., "SAPERE - Space Advanced Project for Excellence in Research and Enterprise", DTA/20-2015.

[8]Manente, M., et al., "Numerical simulation of the Helicon double layer thruster concept", *AIAA Paper*, 2007-5312.

[9]Rao, S., and Singh, N., "Numerical simulation of current-free double layers created in a helicon plasma device", *Physics of Plasmas*, Vol. 19, No.9, 093507, 2012.

[10]Pavarin D., et al., "Development of plasma codes for the design of mini-helicon thrusters", *Proceedings of 32nd Int. Electric Propulsion Conference*, Wiesbaden, Germany, 2011.

[11]Melazzi, D., and Lancellotti, V., "ADAMANT: a surface and volume integral-equation solver for the analysis and design of helicon plasma sources", *Computer Physics Communications*, Vol. 185, 2014, pp. 1914–1925.

[12]Magarotto, M., et al., "Numerical Model of an Helicon Plasma Source for Space Propulsion Application" *Proceedings of 7th European Conference for Aerospace Sciences*, EUCASS 2017

[13]Jasak, H., Jemcov, A., Tukovic, Z., "OpenFOAM: A C++ library for complex physics simulations", *International workshop on coupled methods in numerical dynamics*. Vol. 1000. IUC Dubrovnik, Croatia, 2007.

[14]Cichocki, F., et al., "Fluid vs PIC Modeling of a Plasma Plume Expansion", 2015

[15]Merino, M., and Ahedo, E., "Two-dimensional quasi-double-layers in two-electron-temperature, current-free plasmas", *Physics of Plasmas*, Vol. 20, No. 2, 023502, 2013.

[16]Singh, N., "Current-free double layers: A review", *Physics of Plasmas*, Vol. 18, No. 12, 122105, 2011.

[17]http://www.comsol.com

[18]Dular, P., and Christophe, G., "GetDP: A general environment for the treatment of discrete problems", 1997.

[19]Langdon, A. B., and Lasinski, B. F., "Electromagnetic and relativistic plasma simulation models", *Methods in Computational Physics*, Vol 16, 1976, pp. 327–366.

[20]Ahedo, E., and Navarro-Cavalle, J., "Helicon thruster plasma modeling: Two-dimensional fluid-dynamics and propulsive performances", *Physics of Plasmas* Vol. 20, No. 4, 043512, 2013.

[21]Fiala, A., Pitchford, L., Boeuf, J. P., "Two-dimensional, hybrid model of low-pressure glow discharges", *Phys Rev*, Vol. 49, No. 6, pp. 5607–24, 1994.

[22]Lieberman, M. A., Lichtenberg, A. J., "Principles of plasma discharges and materials processing", *John Wiley & Sons*, 2005.

[23]Chicheportiche, A., et al., "Ab initio transport coefficients of Ar+ ions in Ar for cold plasma jet modeling", *Physical Review*, Vol. 89, No. 6, 063102, 2014

[24]Mikellides, I. G., et al., "Hollow cathode theory and experiment. II. A two-dimensional theoretical model of the emitter region" *Journal of Applied Physics*, Vol. 98, No. 11, 113303, 2005.